COBEM 2021 26th International Congress of Mechanical Engineering
November 22-26, 2021, Virtual Congress, Brazil

COB-2021-0757 TRANSVERSE VIBRATIONS OF A TURBOJET ROTOR SUBJECTED TO CRUISE MISSILE FLIGHT MANEUVERS

Sâmela Fernandes Pereira de Lima
Master Course of the Postgraduate Program in Space Sciences and Technologies, Technological Institute of Aeronautics, Department of Science and Aerospace Technology, São José dos Campos, SP, Brazil
samelafplima@hotmil.com

Carlos d'Andrade Souto
Division of Integration and Tests, Institute of Aeronautical and Space, Department of Science and Aerospace Technology, São José dos Campos, SP, Brazil
soutocds@fab.mil.br

Abstract. *Cruise missiles are guided missiles that usually have the configuration of a small aircraft propelled by a turbojet engine. Many of these missiles have sophisticated guidance systems and are designed to fly at low altitude following the terrain elevations in order to hinder detection by radar and thus adopt a path with many changes of direction and altitude. The maneuvers performed by an aircraft subject all its embedded components to intense dynamic loading. The objective of this work is to estimate the effect of the maneuvers performed on a typical cruise missile trajectory on the rotor dynamic behavior of a low power turbojet engine. To carry out this study, an implementation of the finite element method for the analysis of flexible rotors and hard disks was developed in a routine written with a numerical computing software.*
Keywords: *cruise missile, rotor, vibration.*

1. INTRODUCTION

Rotating machines are widely used in various fields of engineering today. They are systems made up of an element capable of rotating around its own axis (rotor) and a fixed element that surrounds the rotor (stator). These machines require special care both in their design and operation due to possible problems related to the presence of a rotating component: mechanical vibration (which can cause damage to the structure, reduce useful life and even cause catastrophic system failures).

In an ideal rotor the rotation axis and the symmetry axis are coincident and, therefore, all energy supplied to the system is converted into rotation. However, in practice, even in rotors built with very tight geometric tolerances, there are some geometric imperfections that cause the rotor to deviate from the ideal condition and part of the rotational energy is converted into transverse movements (which can still be accentuated with increased speed angle and energy input into the system).

This work is applied to the analysis of transverse vibrations of rotary machines embedded in cruise missiles. The setting of a cruise missile is very similar to a small aircraft powered by a turbojet engine, but these missiles are capable of maneuvering with higher load factors and can adopt a trajectory with many changes in direction and altitude (Ekutekin, 2007), resulting in higher accelerations in its payload and other on-board components.

Generally, in the design phase of rotating machines, its bases are considered to be fixed. However, a flight that performs multiple maneuvers provides an extremely complicated operating environment for a rotor system that is subjected to external forces, excitations and gyroscopic moments during operation (Chen *et al.*, 2020); and for this reason, it is important to analyze the dynamic characteristics of the rotor during a maneuvered flight. For this research was developed a finite element method implementation, in a numerical computation routine for analysis of flexible rotors, considering a simplified mathematical model that assumes the hypothesis that the analyzed missile trajectory is contained in the vertical plane.

2. DEVELOPMENT

A classic form of mathematical modeling of the transverse vibrations of a rotor is to obtain the equations of motion from the application of the Lagrange equation (Eq. 1). From there, a system of matrix equations that describes the dynamic behavior of a continuous system (the rotor) is obtained through the finite element method and some numerical methods are then used to solve these equations and obtain the system's-free vibrations and dynamic response to forces applied on the shaft.

$$\frac{d}{dt}\left(\frac{\partial T}{\partial \dot{q}_i}\right) - \frac{\partial T}{\partial q_i} + \frac{\partial U}{\partial q_i} = Fq_i, \tag{1}$$

Where: T is the kinetic energy, U is the potential energy, q_i is a generalized coordinate and Fq_i is an applied force.

For the analysis, the rotor-bearing assembly is considered as a flexible shaft with disks treated as rigid, described as points with mass and inertia. With the system discretized by the finite element method, the development of expressions of kinetic energy and potential energy (deformation) for shaft element, disks (mass points) and unbalanced masses allows obtaining the equations of motion of each element as shown in (Lalanne and Ferraris, 1990). Once the equations for each element are obtained, the global matrix equation (Eq. 2) of rotor motion that describes the behavior of the system as a whole is assembled.

$$[M]\{\ddot{x}(t)\} + [D(\Omega)]\{\dot{x}(t)\} + [K]\{x(t)\} = \{f(t)\}, \tag{2}$$

Where $[M]$ is the mass matrix, $[D(\Omega)]$ is a matrix composed of the sum of damping matrix [C] and the gyroscopic matrix [G(Ω)] so that $[D(\Omega)]$ = [C]+ [G(Ω)], Ω is angular speed, $[K]$ is the stiffness matrix, $\{x(t)\}$ is the nodal displacements vector given by Eq. 3, and $\{x(t)\}$ is the nodal forces vector given by:

$$\{x(t)\} = \{u_1 v_1 \theta_1 \Psi_1 u_2 v_2 \theta_2 \Psi_2 u_3 v_3 \theta_3 \Psi_3\}, \tag{3}$$

In order to solve the homogeneous version of Eq. (2) and obtain the natural frequencies and modes of the system, it is necessary to solve an eigenvalues and eigenvectors problem. In order to use more efficient algorithms to solve the eigenvalues problem of the homogenous version of equation Eq. (2), it should be transformed into a first-order matrix equation in state space format displayed in Eq. (4).

$$[A]\{\dot{q}\} + [B]\{q\} = \{F\}, \tag{4}$$

Where the matrices $[A]$ and $[B]$ are given by the Eqs. (5) and (6).

$$[A] = \begin{bmatrix} [M] & [0] \\ [0] & -[K] \end{bmatrix}, \tag{5}$$

$$[B] = \begin{bmatrix} [D(\Omega)] & [K] \\ [K] & [0] \end{bmatrix}, \tag{6}$$

Then the homogeneous version of Eq. (4) can be solved by using algorithms for symmetric matrices and the natural frequencies for each angular speed can be calculated.

For real rotors (even those built with great geometric precision) the center of mass and the center of rotation are never exactly coincident. Thus, an unbalance must be added to the model. In a model with a flexible shaft and hard disks, the unbalance is concentrated on the disks. Then, an unbalanced mass m is placed at a distance e from the rotation center of a disk, as shown in Fig. 1.

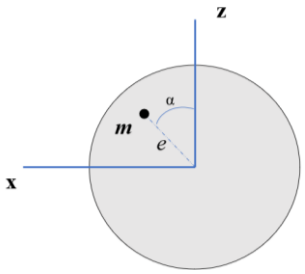

Figure 1. Disk with mass unbalance.

The forces generated due to the movement of this unbalanced mass are given by the Eq. 7 (Lalanne and Ferraris, 1990).

$$\{F\} = \{F_S\} sin(\Omega t) + \{F_C\} cos(\Omega t), \tag{7}$$

Where the vertical and horizontal components of the excitation due to unbalance are applied in the u_1 and v_1 degrees of freedom respectively. The force vectors are shown in Eqs. (8) and (9).

$$\{F_s\} = \{me\Omega^2 \sin(\Omega t) \;\; 0 \;\; 0 \;\; 0 \;\; 0 \;\; 0 \;\; 0 \;\; 0\}, \tag{8}$$

$$\{F_c\} = \{0 \;\; me\Omega^2 \cos(\Omega t) \;\; 0 \;\; 0 \;\; 0 \;\; 0 \;\; 0 \;\; 0\}, \tag{9}$$

The response to this external force will have the same form as Eq. (7):

$$\{Q\} = \{Q_S\}sin(\Omega t) + \{Q_C\}cos(\Omega t), \tag{10}$$

By replacing the Eq. (10) and Eq. (7) in the rotor global equation, the vectors $\{Q_S\}$ and $\{Q_c\}$ can be obtained.

$$\begin{Bmatrix} Q_S \\ Q_c \end{Bmatrix} = \begin{bmatrix} [K] - \Omega^2[M] & -\Omega[D(\Omega)] \\ \Omega[D(\Omega)] & [K] - \Omega^2[M] \end{bmatrix}^{-1} \begin{Bmatrix} F_s \\ F_c \end{Bmatrix}, \tag{11}$$

Due to the maneuvers that a missile performs during its trajectory, the entire system is subjected to high dynamic loads. For the model analyzed in this work, the final phase of the missile trajectory is discussed, where the speeds (angular and of the aircraft) are considered as constant and the curve performed during the flight and its effects are analyzed below.

2.1 Response to forces arising from missile maneuvers

In Fig. 2 is shown the rotor at its base (fixed to the missile in this case) and the coordinate systems used in this work.

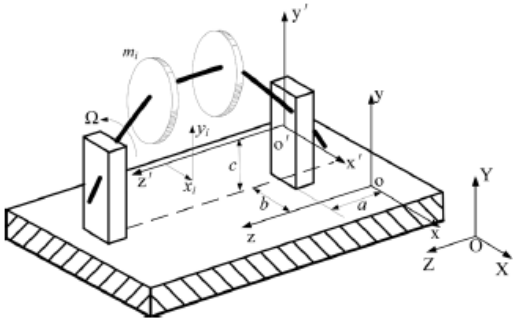

Figure 2. Rotor, its base and coordinate systems. Extracted from (Zhansheng *et al*, 2015).

In the figure, the missile movements are described in relation to the inertial system fixed to the ground OXYZ and the rotor transverse movements (given by Eq. 12) are described in relation to the o'x'y'z' system. Furthermore, the rotor position in relation to the base is described in the oxyz coordinate system and the mass of the i-th disk is m_i and the eccentricity of the respective unbalanced mass is e_i.. The equations of motion considering the forces caused by the maneuvers are given by (Zhansheng *et al*, 2015):

$$M_i\ddot{q}_i + \left(C_i + G_i + C_{J,i}\right)\dot{q}_i + \left(K_i + K_{J,i}\right)q_i = F_{u,i}(t) + F_{g,i}(t) + F_{J,i}(t), \tag{12}$$

Where the matrices M_i, M_i, M_i and M_i are given by the Eqs. (13) to (16).

$$M_i = \begin{bmatrix} m_i & 0 & 0 & 0 \\ 0 & m_i & 0 & 0 \\ 0 & 0 & I_{d,i} & 0 \\ 0 & 0 & 0 & I_{d,i} \end{bmatrix}, \tag{13}$$

$$G_i = \begin{bmatrix} 0 & 0 & 0 & 0 \\ 0 & 0 & 0 & 0 \\ 0 & 0 & 0 & I_{p,i}\Omega \\ 0 & 0 & -I_{p,i}\Omega & 0 \end{bmatrix}, \tag{14}$$

$$C_{J,i} = \begin{bmatrix} 0 & -2m_i\dot{\theta}_{J,z} & 0 & 0 \\ 2m_i\dot{\theta}_{J,z} & 0 & 0 & 0 \\ 0 & 0 & 0 & -2I_{d,i}\dot{\theta}_{J,x}\theta_{J,y} \\ 0 & 0 & -2I_{d,i}\dot{\theta}_{J,x}\theta_{J,y} & I_{d,i} \end{bmatrix}, \tag{15}$$

$$K_{J,i} = \begin{bmatrix} -m_i(\dot{\theta}_{J,y}^2 + \dot{\theta}_{J,z}^2) & m_i(\dot{\theta}_{J,x}\dot{\theta}_{J,y} - \ddot{\theta}_{J,z}) & 0 & 0 \\ m_i(\dot{\theta}_{J,x}\dot{\theta}_{J,y} + \ddot{\theta}_{J,z}) & -m_i(\dot{\theta}_{J,x}^2 + \dot{\theta}_{J,z}^2) & 0 & 0 \\ 0 & 0 & 0 & 2I_{d,i}(\ddot{\theta}_{J,x}\theta_{J,y} + \dot{\theta}_{J,x}\dot{\theta}_{J,y}) \\ 0 & 0 & 0 & 0 \end{bmatrix}, \tag{16}$$

The forces $F_{u,i}$ and $F_{J,i}$ are shown in Eqs. (17) and (18).

$$F_{u,i}(t) = \begin{bmatrix} m_i e_i \Omega^2 \cos(\Omega t + \varphi_{i,0}) \\ m_i e_i \Omega^2 \cos(\Omega t + \varphi_{i,0}) \\ 0 \\ 0 \end{bmatrix}, \tag{17}$$

$$F_{J,i}(t) = \begin{bmatrix} A \\ B \\ D \\ E \end{bmatrix}, \tag{18}$$

The nodal displacements vector is described in Eq. (19).

$$q_i = \{x_i \;\; y_i \;\; \theta_{x,i} \;\; \theta_{y,i}\}, \tag{19}$$

Where x_i and y_i represent the horizontal and vertical displacements of the i-th disk; $\theta_{x,i}$ and $\theta_{y,i}$ represent the rotations around the horizontal and vertical axis.

Considering that the missile, in its trajectory, does not suffer transverse displacements in its main displacement (Z axis) and angular displacements around the Y and Z axis, for the linear displacements of the missile, we have:

$$X_j = \dot{X}_j = 0 \tag{20}$$

Where the subscript *j* indicates the base movements (missile) in relation to the inertial system fixed to the ground. And for its angular displacements:

$$\theta_{j,y} = \theta_{j,z} = \dot{\theta}_{j,y} = \dot{\theta}_{j,z} = \ddot{\theta}_{j,y} = \ddot{\theta}_{j,z} = 0, \tag{21}$$

For the angular speed of the maneuver, it is necessary that:

$$\ddot{\theta}_{j,z} = \omega_{maneuver} = 0, \tag{22}$$

Therefore, the elements *A*, *B*, *D* and *E* of Eq. (18) are given by the Eqs. (23) to (26).

$$A = 0, \tag{23}$$

$$B = -m_i\left(\ddot{Y}_j - \omega_m \dot{Z}_j\right) + m_i\, c\, \omega_m^2 + m_i\, e_i\, \omega_m^2\, sen(\Omega t) - m_i\, g\, cos(\omega_m t), \tag{24}$$

$$D = 0, \tag{25}$$

$$E = I_p \Omega \omega_m, \tag{26}$$

Where $\ddot{Y}_j$ is the missile acceleration in Y axis, $\ddot{Z}_j$ is the missile velocity in Z axis, m_i is the disk mass, e_i represents the unbalance, and ω_m is the missile angular speed during maneuver. The trajectory model, extracted from (Hou *et al*, 2016) and considered at this analysis can be observed in Fig. 3.

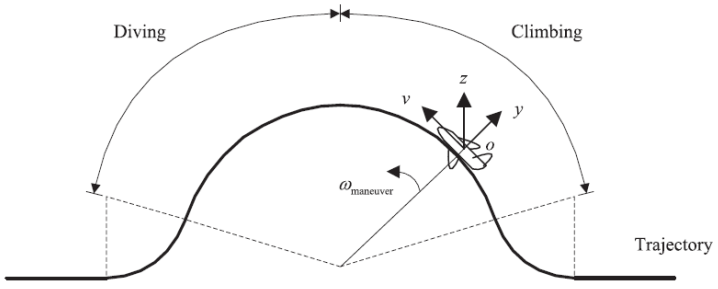

Figure 3. Maneuver trajectory. Extracted from (Hou *et al*, 2016).

2.2 Rotor specifications of the analyzed model

The rotor analyzed in this paper is a turbojet, described in (Creci, 2011), TAPP5000 used in aeronautical applications involving unmanned aerial vehicles. It is designed to generate 5kN of thrust and operate in a speed range from 22520 to 28550 rpm. In Fig. 4, the rotor-dynamic model with all geometric dimensions (in meters) is presented. The numbers shown on the shaft correspond to the nodes of the finite element model implemented in the MATLAB routine.

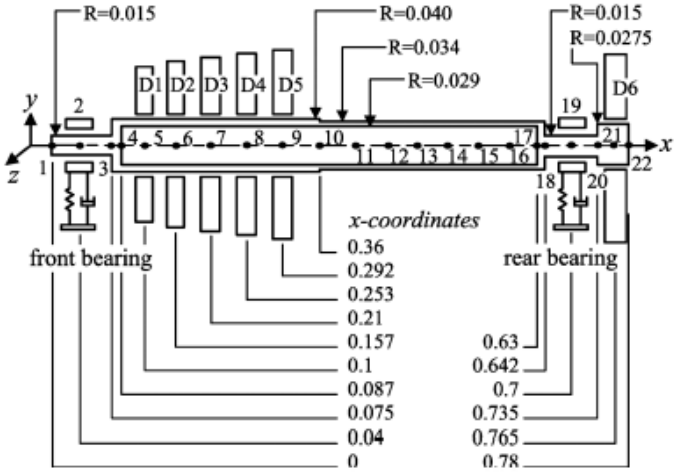

Figure 4. Rotor-dynamic model. Extracted from (Creci, 2012).

Where the disks 1 to 5 (D1, D2, D3, D4 and D5) are the compressor disks, the disk 6 (D6) is the turbine disk and its properties are shown in Table 1 (Creci, 2012).

Table 1. Specifications and properties of disks.

Property	**D1**	**D2**	**D3**	**D4**	**D5**	**D6**
Specific Mass [kg/m^3]	2830	2830	2870	4430	4430	8000
Width [m]	0.02	0.02	0.02	0.02	0.02	0.03
Inner Diameter [m]	0.08	0.08	0.08	0.08	0.08	0.055
Outer Diameter [m]	0.19	0.21	0.23	0.24	0.25	0.25

The stiffness and damping properties are shown in Table 2 (Creci, 2012). Also, in both bearings, the properties are the same in the vertical and horizontal directions and there are no couplings in these directions; that is: $C_{yy} = C_{zz}$, $K_{yy} = K_{zz}$; e $C_{yz} = C_{zy=} K_{yz} = K_{zy} = 0$.

Table 2. Specifications and properties of disks.

	Front		**Back**	
Speed [rpm]	**Stiffness [N/m]**	**Damping [Ns/m]**	**Stiffness [N/m]**	**Damping [Ns/m]**
0	1.37x10^7	39.3	2.94x10^6	9719.7
5000	1.37x10^7	33.4	2.94x10^6	9719.7
10060	1.37x10^7	19.4	5.30x10^6	7855.7
15000	1.37x10^7	13.5	7.16 x10^6	6055.9
20000	1.37x10^7	9.3	8.44 x10^6	4216.1
25000	1.37x10^7	7.0	10.5 x10^6	3352.2
30000	1.37x10^7	5.1	12.5 x10^6	2441.2

In addition, values of 205GPa were used for the AISI4340 modulus of elasticity, 0.29 for the Poisson's coefficient and 7850 kg/m^3 for the shaft element specific mass.

3. RESULTS

Through the computational implementation in the MATLAB numerical programming platform, performed by the authors, the results related to the rotor displacements influenced by the maneuvers were analyzed in different operational situations:

1. During a trajectory in level flight, where no maneuver effects are present.
2. During an incomplete trajectory where the missile moves from level flight to make an ascent maneuver (to reach the transition point) and remains at this point in level flight, not completing the dive to the target.
3. During a full trajectory, where the missile performs ascent and descent maneuvers to the target.

In Fig 5 the horizontal and vertical displacement of the center of the disk are presented. Due to the presence of unbalance, the rotor disc centers will always have transverse displacements while the rotor is rotating. Consequently, the rotor discs will show changes in their transverse displacements.

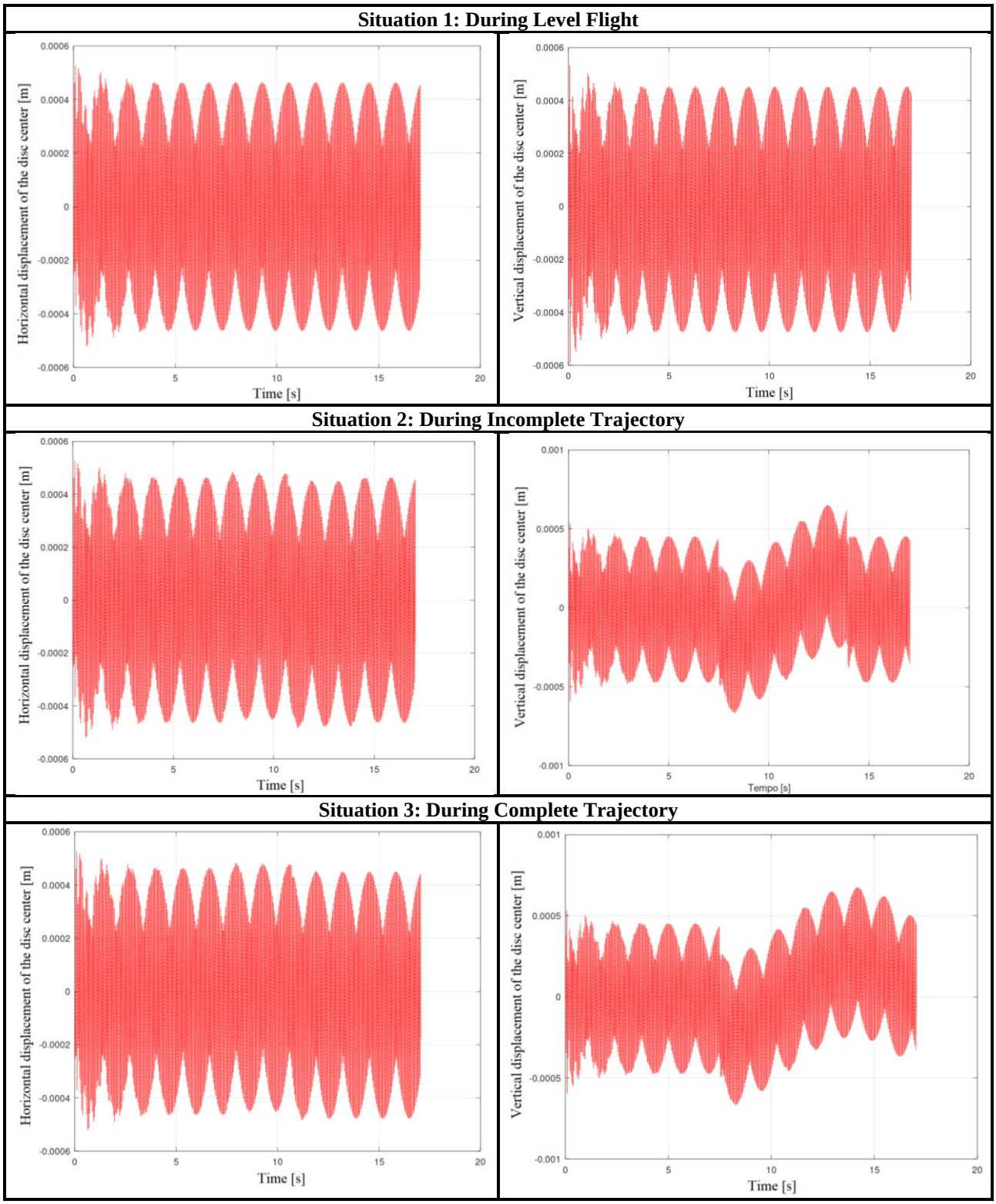

Figure 5. Horizontal and vertical displacement of the center of the disk.

In the two figures in the first row of Fig. 5, the displacement amplitudes remain constant, as it is a level flight without the influence of maneuvers and, therefore, there is no change in displacements. In the figures of the second row, it is possible to analyze the displacements during the trajectory without a dive to the target. Between the time interval of 6 to 14 seconds, there is a variation of displacements caused by the maneuver, and after this interval, the displacements return to their previous form (of level flight). In the figures on the last row, it is possible to observe a change in displacement values from the moment of 6 seconds to the end of the trajectory, from the ascent maneuver to its transition point and dive to reach the target.

The behavior of the rotor during maneuvers can also be observed in the displacement orbits from the center of the turbine disk (disk 6) in Fig. 6. The figure shows the orbits referring to the complete trajectory followed by the missile.

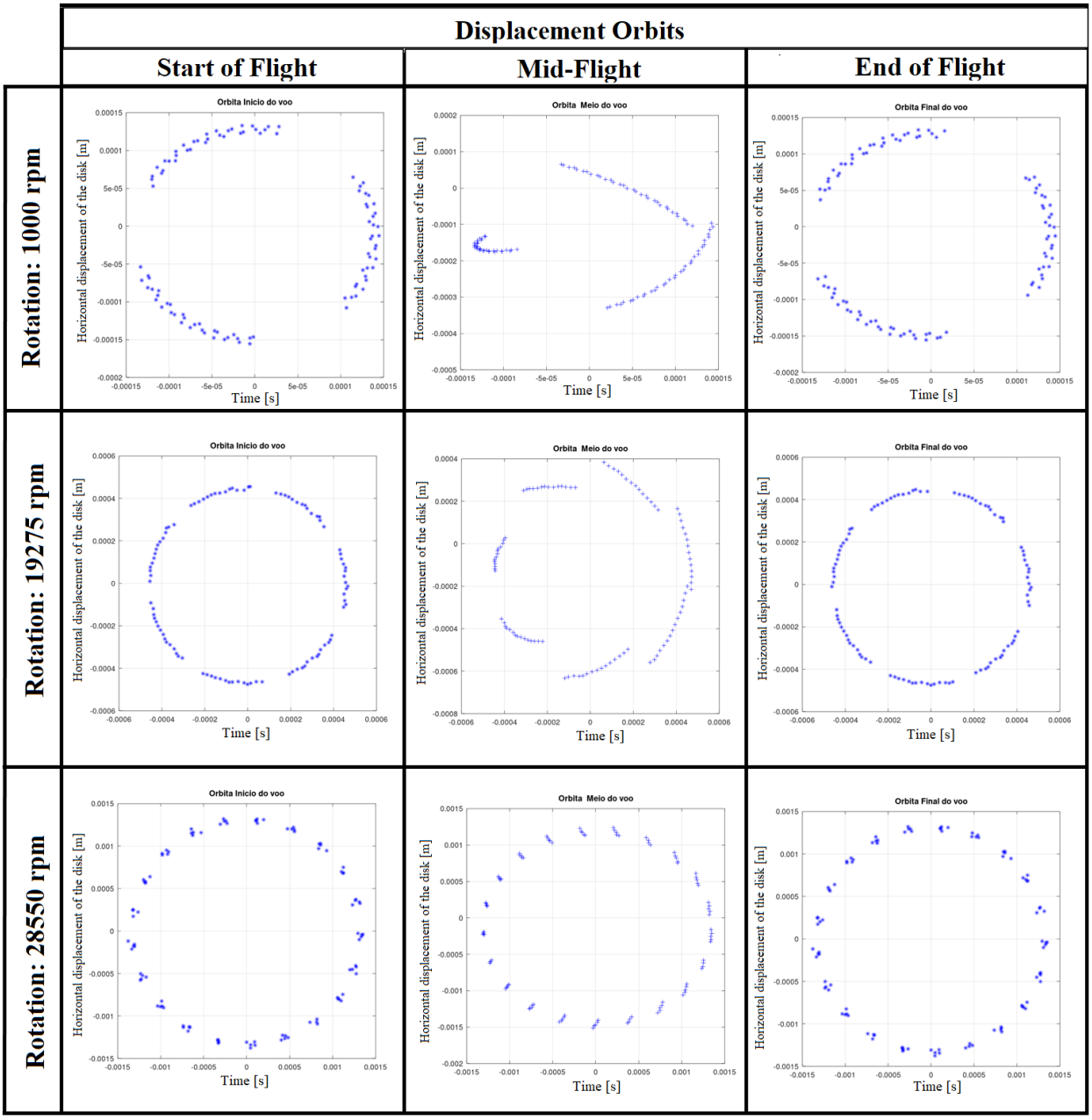

Figure 6. Disk displacement orbits along the trajectory.

These orbits show the horizontal displacement positions of the disk as a function of time. Results are plotted for three different operating ranges: 10000 rpm, 19275 rpm and 28550 rpm (maximum operating speed). In addition, orbits in different phases of the trajectory are presented: start of flight, mid-flight and end of flight; in order to obtain a simulation of the behavior of the disk along the trajectory.

In the Fig 6, it is possible to observe that larger changes occur in the displacements of the disk center, especially during mid-flight, resulting from the maneuvers performed by the missile. The orbits present greater variations in the

displacements resulting from the maneuvers. Furthermore, when the rotor operates at low speeds, the disc tends to have a behavior with greater variation.

4. CONCLUSION

Different operational situations were analyzed through a series of control variables (path type, rotation speed, etc.) and it is possible to see the great influence that the maneuvers have on the operation of the rotor set during your operation.

Considering a level flight, the rotor does not show changes in the vertical displacement. Only a slight difference between horizontal and vertical displacements due to the effect of gravity that tends to shift the equilibrium condition slightly below the x-axis (that occurs in all conditions). In the condition of an incomplete trajectory, the rotor presents vertical displacements in the same time interval in which it performs the maneuvers, returning to its equilibrium condition when it finishes the maneuvers. And, when the missile performs the complete path, the rotor presents changes in the transverse displacements since the beginning of the maneuvers to finish his mission.

Physically, the effects of displacements relate to the normal force acting on the missile. Similarly, when a missile is climbing at high speed, its embedded elements are compressed against the vehicle itself. Therefore, it is as if the rotor were being pushed down (negative vertical displacements) and the same happens in a reverse maneuver (positive displacements for diving in flight).

Just as variations in vertical displacement are highly influenced by maneuvers, so is the shape of the orbits, which is more affected in the intermediate region of flight where the change in the missile's angular velocity is sudden due to the change in direction from one curve to another.

Finally, the study of rotor behavior in various types of trajectories provided useful information for the design of a turbojet onboard an aircraft with high maneuverability.

5. ACKNOWLEDGEMENTS

The authors thank the support of CAPES (PROAP) and thank the '*Coordenação de Aperfeiçomento de Pessoal de Nível Superior'* (CAPES) for the scholarship awarded to the first author.

6. REFERENCES

Chen, X., Gan, X., Ren, G., 2020. "Effect of flight/structural parameters and operating conditions on dynamic behavior of a squeeze-film damped rotor system during diving-climbing maneuver". Shenzhen: Journal of Aerospace Engineering. 31 p.

Creci, G., 2012. "Influência da dinâmica dos mancais na resposta vibratória de uma turbina aeronáutica de 5kN de empuxo". São José dos Campos: ITA.

Creci, G, 2011. "Rotordynamic analysis of a 5-kilonewton thrust gas turbine by considering bearing dynamics". São José dos Campos: Journal Propulsion and Power.

Ekutekin, V., 2007. "Navigation and control studies on cruise missiles". Çankaya: METU. 298 p.

Hou, L., Chen, Y., Cao, Q., Lu, Z., 2016. "Nonlinear vibration analysis of a cracked rotor-ball bearing system during flight maneuvers". Harbin: ELSEVIER. pp. 515 – 528.

Lalanne, M., Ferraris, G., 1990. "Rotordynamics prediction in engineering". Lyon: Wiley.

Lima, S. F. P.; Souto, C. d'A, 2020. "Dynamic analysis of the set rotor-bearings of a small power turbojet". São Paulo: SAE. 6 p.

Zhansheng, L., Guanghui, Z., Ruixian, M., Shupeng, L., 2015. "Nonlinear dynamic characteristics of journal bearing-rotor system considering the pitching a rolling motion for marine machinery". Harbin: Journal of Engineering for the Maritime Environment. Vol. 229 (1) 95-107.

7. RESPONSIBILITY NOTICE

The authors are the only responsible for the printed material included in this paper.